

Session Topic Number: 31

Keywords: *progressive failure, damage modeling, non-crimp fabric composites*

Progressive Damage Modeling of Notched Composites

Venkat Aitharaju¹, Satvir Aashat², Hamid Kia¹

Arunkumar Satyanarayana³, Philip Bogert³

¹General Motors Global Research and Development, Warren, MI 48092.

² Engineering Technology Associates, Troy, MI 48083.

³ NASA Langley Research Center, Hampton, VA 23681.

*Corresponding Author: Venkat.aitharaju@gm.com

ABSTRACT

There is an increased interest in using non-crimp fabric reinforced composites for primary and secondary structural weight savings in high performance automobile applications. However, one of the main challenges in implementing these composites is the lack of understanding of damage progression under a wide variety of loading conditions for general configurations. Towards that end, researchers at GM and NASA are developing new damage models to predict accurately the progressive failure of these composites. In this investigation, the developed progressive failure analysis model was applied to study damage progression in center-notched and open-hole tension specimens for various laminate schemes. The results of a detailed study with respect to the effect of element size on the analysis outcome are presented.

INTRODUCTION

Usage of advanced fibrous composites in the structural areas of the automobile can minimize the vehicle weight and thus achieve improved fuel economy and reduce emissions. However, failure mechanisms and damage evolution of composite materials pose significant challenges in accurate prediction of load carrying capacity and are one of the major barriers in large scale implementation of composite materials in automobiles. The failure modes of the composites include fiber pull out and breakage or kinking, matrix cracking, fiber/matrix interface shear failure and delamination between the layers. The type of failure in a composite is highly dependent on the nature of loading, lay-up, and geometric conditions of the composite. In the case of an automotive assembly made of composite materials, one cannot avoid the presence of holes or cutouts, which include stress concentrations and can reduce the strength significantly. Notched strength is hence one of the design drivers for composite structure in load bearing areas. Several researchers studied the strength of notched composites through experiments, empirical methods and computational numerical methods. Experiments performed by Waddoupsand [1] showed that the tensile strength of notched quasi-isotropic laminates with thin plies decreased as the circular hole size is increased. The phenomenon of "hole size effect" was explained as the propagation of subtle damage modes occurring at the ply interface level. The effect of these local damage modes on small size notched

specimens is significant and complete failure of the composite can occur at much lower strength compared to specimens where the hole diameter to width ratio is small. Contrary to this fact, several researchers also reported that increasing the hole diameter while keeping the width constant increased the strength and they attributed this effect to the delamination failure relieving some of the high stress at the hole boundary [2,3]. This phenomenon has been demonstrated numerically by Satyanarayana [4] for a notched specimen. Caminero [5] used digital image correlation (DIC) techniques to assess the damage taking place in composite plates with an open hole loaded in tension. He compared the stress concentration factors obtained analytically using the elastic solution of an infinite orthotropic plate containing a hole with the experimental results obtained from DIC measurements.

Whitney, Nuismer [6] and Pipes [7] developed an empirical approach to determine the final failure load using the point stress and averaged stress methods. In the point stress method, the failure of the composite is assumed to occur when the stress at a characteristic distance away from the stress concentration reaches the un-notched strength of laminate. In the average stress method, the failure is assumed to occur when the average stress over the characteristic length reaches the un-notched strength of the laminate. However, the characteristic distance of the composite is highly dependent on the notch size and the laminate orientation and cannot be used to predict the failure strength of the composite from one laminate system to another.

Among the computational methods, methods based on stress intensity factors (SIF) have been used to predict the crack growth and ultimately the failure load of the composites. The J-integral method was applied by Rice [8] to calculate the SIF of a composite with cracks to predict the crack growth by computing the stress and strain at a series of internal points around the crack. However, this procedure is computationally very expensive. In parallel, several progressive failure analysis (PFA) methods based on the continuum damage mechanics were also developed in the literature to model the damage initiation, stiffness degradation behavior after the first ply failure, and ultimately final failure of the composite. The PFA methods based on the continuum damage mechanics have several advantages over other methods and can be easily implemented in the conventional finite element framework. However, during the PFA, the composites invariably meet the strain localization problem for geometrically discontinuous composite structures with holes, notches and cutouts. During the localization, the strain fields which are initially smooth will suddenly give rise to highly localized fields with high gradients, leading to an ill-posed boundary value problem. The PFA simulation in which failure is analyzed at the integration points, usually does not take in to account the amount of material that is failed. Ignoring the amount of failed material under each of the integration points results heavy dependency of the predicted load with the mesh size. This can cause a huge amount of uncertainty in predicted results and weaken the confidence in the analysis. To remedy the mesh sensitivity on the predicted results, a few approaches were developed. They are broadly categorized into two main categories, scaling the strength to failure or scaling the failure strain such that the energy dissipated is constant, and nonlocal formulations based on characteristic length. Satyanarayana et.al [9] developed an approach of scaling the strength for different element sizes and a higher order polynomial function was constructed between strength and element area. Kenik et.al [10] modified the slope of the softening portion of the stress-strain curve after the failure to eliminate the mesh size effects. Bazant [11] developed an approach to deal with this spurious mesh dependency using a smeared

crack band model that introduced a characteristic element length into the formulation of the damage evolution.

The objective of the paper is to develop a mesh independent solution for the intra and inter layer damage formulations developed previously by the authors [12]. The strength scaling procedure developed in [11] will be implemented. The developed framework will be tested by simulating notched and open-hole samples. The following sections of the paper present details of the material system, the Complete Stress Reduction (COSTR) progressive damage model, and experiments and simulations of the center-notched and open hole tension samples followed by brief conclusions.

MATERIAL SYSTEMS FOR THE STUDY

An eight layer carbon fiber non-crimp fabric with quasi-isotropic layup (0/-45/45/90/90/45/-45/0) from Sigmatech was used in the present study. The fibers are of T700 grade. An epoxy resin developed internally in GM to achieve faster curing times and higher toughness was used. The volume fraction of carbon fiber was determined to be close to 48%. Several flat square plaques of length 444.5 mm were molded using resin transfer molding. Flat samples for tension, three-point bend experiments were cut from the plaques and made for material characterization. Following ASTM standards, material characterization experiments were performed to generate the data to determine some of the properties of the composite in tension, compression and shear. However, a few of the composite properties were generated using micromechanics models from Autodesk software. Table I provides the material properties of the composite material system. Material characterization for Inter-layer fracture toughness in mode-1 and mode-2 was also conducted and the data is presented in Table II.

TABLE I. Mechanical properties of NCF Composites

Properties	T700/Epoxy	Description
E_{11} (GPa)	102.0	Young's modulus in fiber direction
E_{22} (GPa)	7.08	Young's modulus in the transverse direction
G_{12} (GPa)	3.16	In-plane shear modulus
X_t (GPa)	1.63	Tensile strength in the fiber direction
X_c (GPa)	1.43	Compressive strength in the fiber direction
Y_t (GPa)	0.068	Tensile strength in the transverse direction
Y_c (GPa)	0.30	Compressive strength in the transverse direction
S_c (GPa)	0.05	In-plane shear strength
ν_{12}	0.28	Poisson's Ratio

TABLE II. Inter-laminar properties and strength data

Properties	Composite	Description
G_{IC} (GPa/mm)	0.00056	Fracture toughness in mode 1
G_{IIC} (GPa/mm)	0.001274	Fracture toughness in mode 2

COSTR DAMAGE MECHANICS MODEL

The progressive damage analysis model used in the present study was based on The Complete STress Reduction (COSTR) damage model, developed for predicting intra-layer failures in [12]. This damage model is interfaced with the LS-Dyna finite element analysis code using a user written subroutine. The Hashin-Rotem failure criteria in the damage mechanics model are expressed in terms of the in-plane stresses.

According to the model, the constitutive stress-strain relations with damage indices were written as

$$\begin{pmatrix} \sigma_{11} \\ \sigma_{22} \\ \sigma_{33} \\ \sigma_{12} \\ \sigma_{23} \\ \sigma_{31} \end{pmatrix} = \begin{pmatrix} C_{11} & C_{12} & C_{13} & 0 & 0 & 0 \\ C_{12} & C_{22} & C_{23} & 0 & 0 & 0 \\ C_{13} & C_{23} & C_{33} & 0 & 0 & 0 \\ 0 & 0 & 0 & C_{44} & 0 & 0 \\ 0 & 0 & 0 & 0 & C_{55} & 0 \\ 0 & 0 & 0 & 0 & 0 & C_{66} \end{pmatrix} \begin{pmatrix} \varepsilon_{11} \\ \varepsilon_{22} \\ \varepsilon_{33} \\ \varepsilon_{12} \\ \varepsilon_{23} \\ \varepsilon_{31} \end{pmatrix} \quad (5)$$

Where

$$\begin{aligned} C_{11} &= (1 - d_f) E_{11} (1 - (1 - d_m) v_{23} v_{23}) \Delta \\ C_{12} &= (1 - d_f) (1 - d_m) E_{22} (v_{12} + v_{12} v_{23}) \Delta \\ C_{13} &= (1 - d_f) (1 - d_m) E_{22} (v_{12} + v_{12} v_{23}) \Delta \\ C_{22} &= (1 - d_m) E_{22} (1 - (1 - d_f) v_{12} v_{21}) \Delta \\ C_{23} &= (1 - d_m) E_{22} (v_{23} + (1 - d_f) v_{12} v_{21}) \Delta \\ C_{33} &= (1 - d_m) E_{22} (1 - (1 - d_f) v_{12} v_{21}) \Delta \\ C_{44} &= 2G_{12} \\ C_{55} &= 2G_{12} \\ C_{66} &= 2G_{12} \\ \Delta &= 1 / (1 - FI^* v_{12} v_{21} - (1 - d_m) v_{23} v_{23} - FI^* v_{12} v_{21} - FI^* 2 v_{12} v_{23} v_{21}) \\ FI &= (1 - d_f) (1 - d_m) \end{aligned} \quad (6)$$

d_f and d_m are the damage indices for the fiber and matrix phases. For details, refer to [12].

CENTER NOTCHED TENSILE SAMPLES – EXPERIMENTS AND SIMULATIONS:

In this section, the effect of element size on the strength prediction of composite laminates with stress concentrations was investigated. In Figure 1, the geometrical details of the tensile samples used in the study are shown. The length of the sample used for testing is 254 mm in length and width of 50.8 mm. An elliptical notch 12.7 mm long was cut at the center of the samples. During preparation of the samples with the notch, care was taken not to cause any delamination damage

around the notch, and this was verified using non-destructive evaluation. Two strain gages were attached to the sample, one near the notch and one away from the notch to measure near and far field strains during the testing.

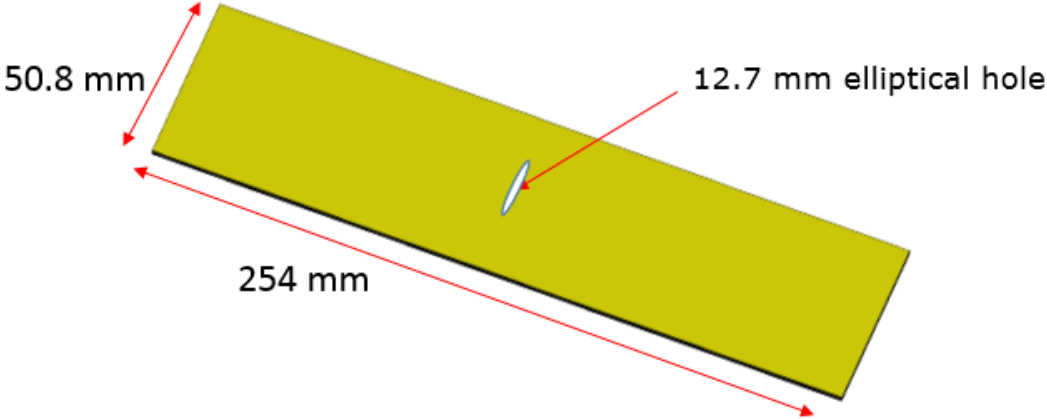


Figure 1. Geometry of the center-notched specimen

Figure 2 shows the damaged samples after testing. The observed failure is more of a brittle fracture at the notch location with fiber pullout.



Figure 2. Center notch samples tested in tension

The experimental load versus strains measured near and away from the notch for all of the specimens are presented in Figure 3. The strain measured at the notch shows a large variation compared to the strain measured near the grip and this could be attributed to the damage along the notch edge.

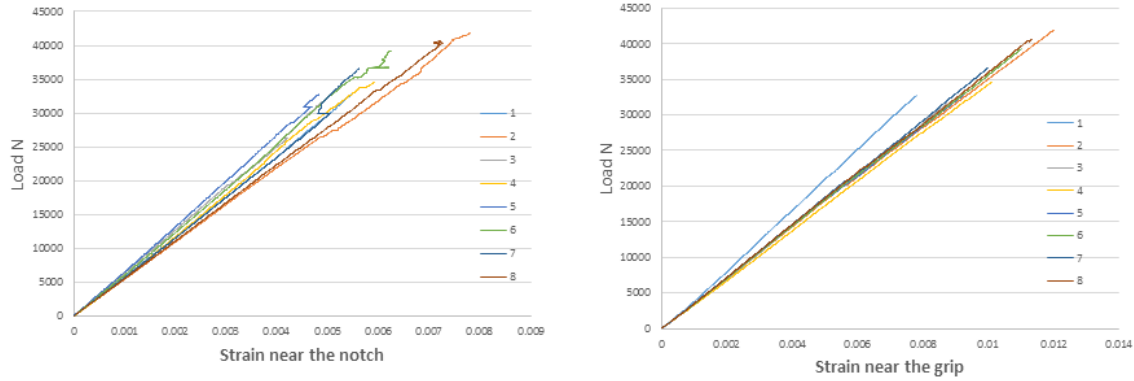


Figure 3. Load versus strain (center-notch) measured for the center-notch specimens

In an effort to develop a damage model that is mesh insensitive, a numerical experiment was conducted by performing progressive failure analyses of the above mentioned center notched specimen with several element sizes. The element size was varied only in the in-plane direction. The center notch models were discretized using 3-D solid elements with one element in the thickness direction for each layer of the composite laminate. The notch in the model was not explicitly modeled but rather simulated with coincident nodes located along the length of the notch. The COSTR damage model which was previously used in simulating crush behavior of a composite tube [12] was used in these analyses to obtain failure loads.

In Figure 4, the predicted load versus strain for various mesh sizes are presented. It can be noticed that using a coarser mesh sizes, the failure loads predicted from simulation are higher compared to finer mesh sizes, showing spurious mesh size effect.

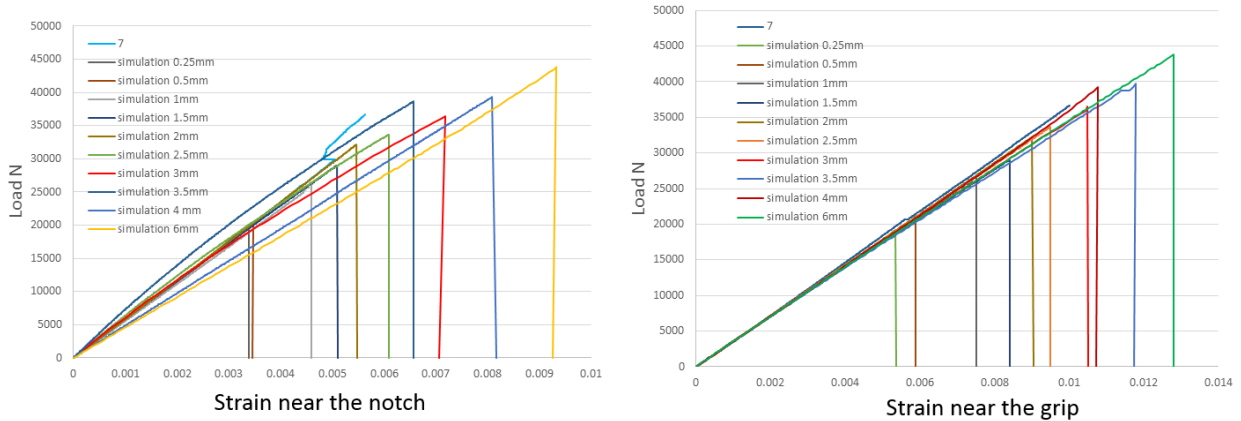


Figure 4. Load versus strain (center-notch) predicted for the center-notch specimens for different mesh sizes

In order to make the damage model mesh regularized (same failure load irrespective of element size), failure loads obtained from progressive failure analysis of various center notch models were recorded and plotted against the element area. A 6th order polynomial curve provided a best fit to these data points and hence was used in identifying a characteristic element area which corresponds

to minimal change in failure load . This element area was used in scaling strengths of the material based on the polynomial curve. Steps involved in the mesh regularization procedure of the damage model is explained in reference [9]. In Figure 5, the results of implementing the mesh regularization procedure is presented where one can observe that the failure loads for the four different mesh sizes collapse into a small range, eliminating any spurious mesh size effect. Also one can notice that the simulated failure load correlates well with the failure load of the test samples.

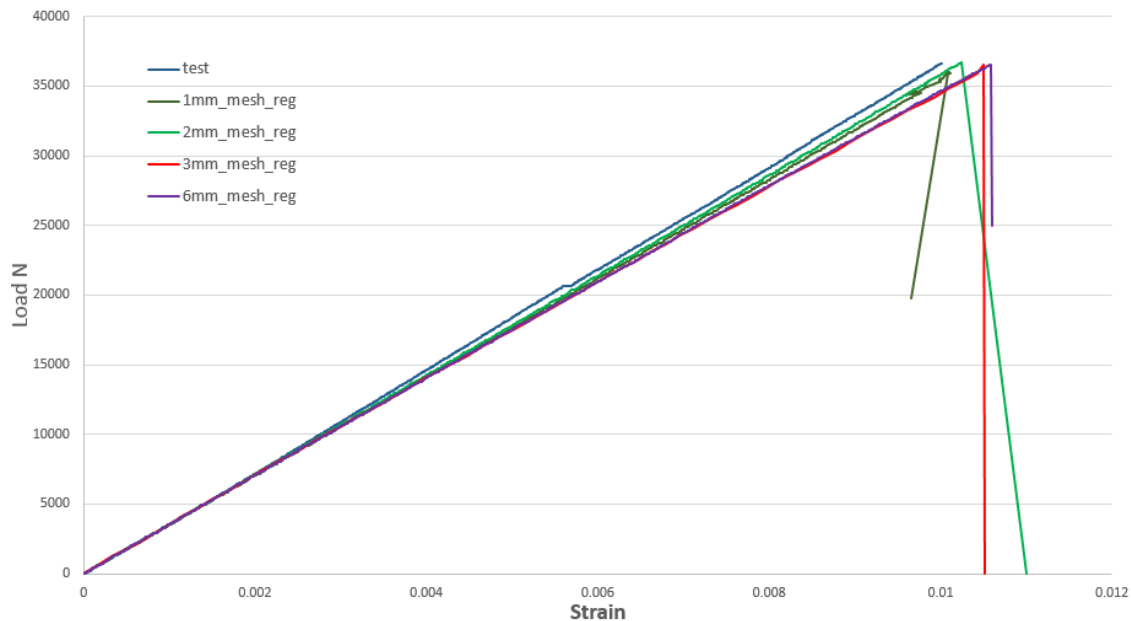


Figure 5. Failure Load Prediction for Various Mesh Sizes using Mesh Regularization Procedure

OPEN-HOLE TENSION TEST

In Figure 6, geometry of the open-hole tension sample following the ASTM standard is presented. A circular hole of 6.35 mm was drilled in the composite specimen and special care was taken to make sure that damage in the composite is limited to the hole boundary. Two lay-ups were investigated.

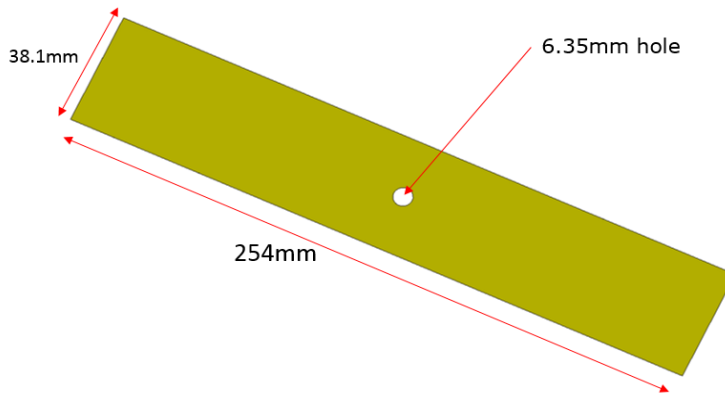


Figure 6. Geometry for the open-hole tension (OHT) specimen

Lay-up 1 - (0/45/-45/90/90/-45/45/0)

The quasi-isotropic samples with lay-up (0/45/-45/90/90/-45/45/0) were tested for tensile loading using an Instron fixture. Figure 7 shows the load versus strain measured from the experiments. For simulations, an element mesh size of 1.0 mm was used to discretize geometry of the sample. One solid element through the thickness was used to model each of the layers of the laminate. Appropriately scaled strength properties for the 1.0 mm mesh size were used. A contact tie break model was defined between each of the layers of the laminate. The parameters for the tie break contact model were defined from the material characterization data collected from G_{IC} and G_{IIC} experiments.

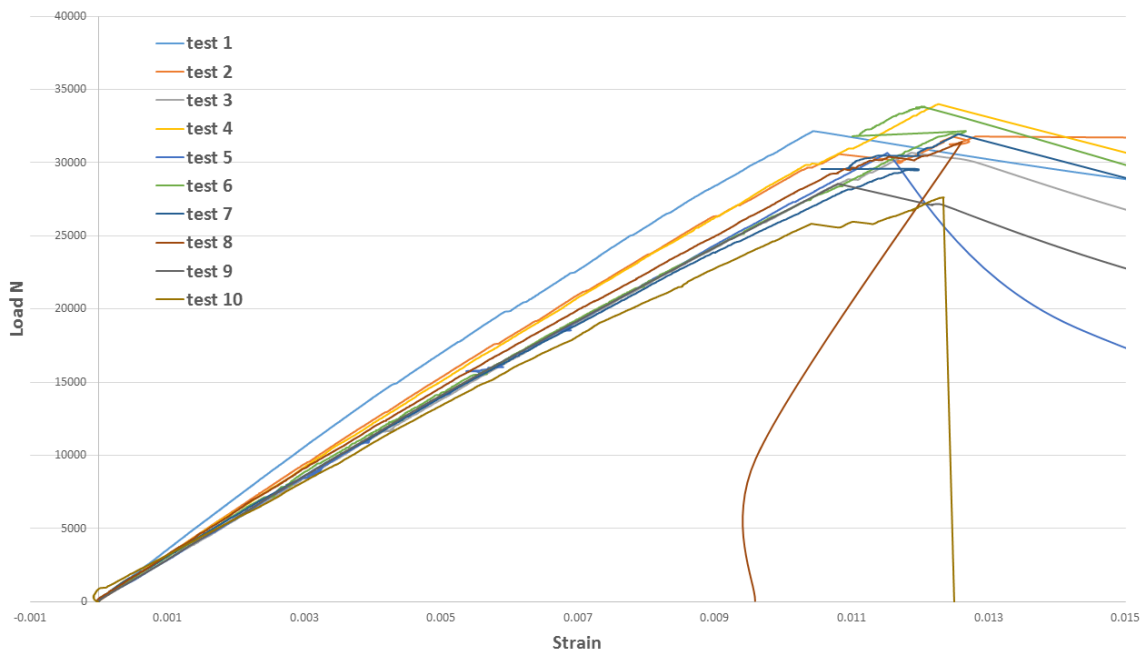


Figure 7. Load versus strain plots for the OHT specimens

Figure 8 shows the failed specimens after testing. The failure in the samples was located at the hole section with fiber pull out. No significant delamination failure was evident. Comparison of

the load versus strain results from the simulation and the experiments are presented in Figure 9. The mean of the experimental results are plotted and compared with the simulation results with and without delamination modeling. The simulation without inter-layer damage model predicts a load of approximately 31 KN for the final failure, whereas the simulation with inter-damage model predicts a maximum failure load of 28 KN. Experiments show a softening of the load versus strain plot at a strain of 1.1% , whereas the simulation shows softening at 0.85% of strain. This softening is attributed to the delamination failure in the sample. Current simulation predicts delamination earlier compared to the experiment and thus finally predicts a little lower peak load compared to the experiment. A good correlation was obtained between the simulation with delamination model and experiment, yielding a small difference in peak load.



Figure 8. Failed specimens of Open Hole Tension Test (Lay-up 1)

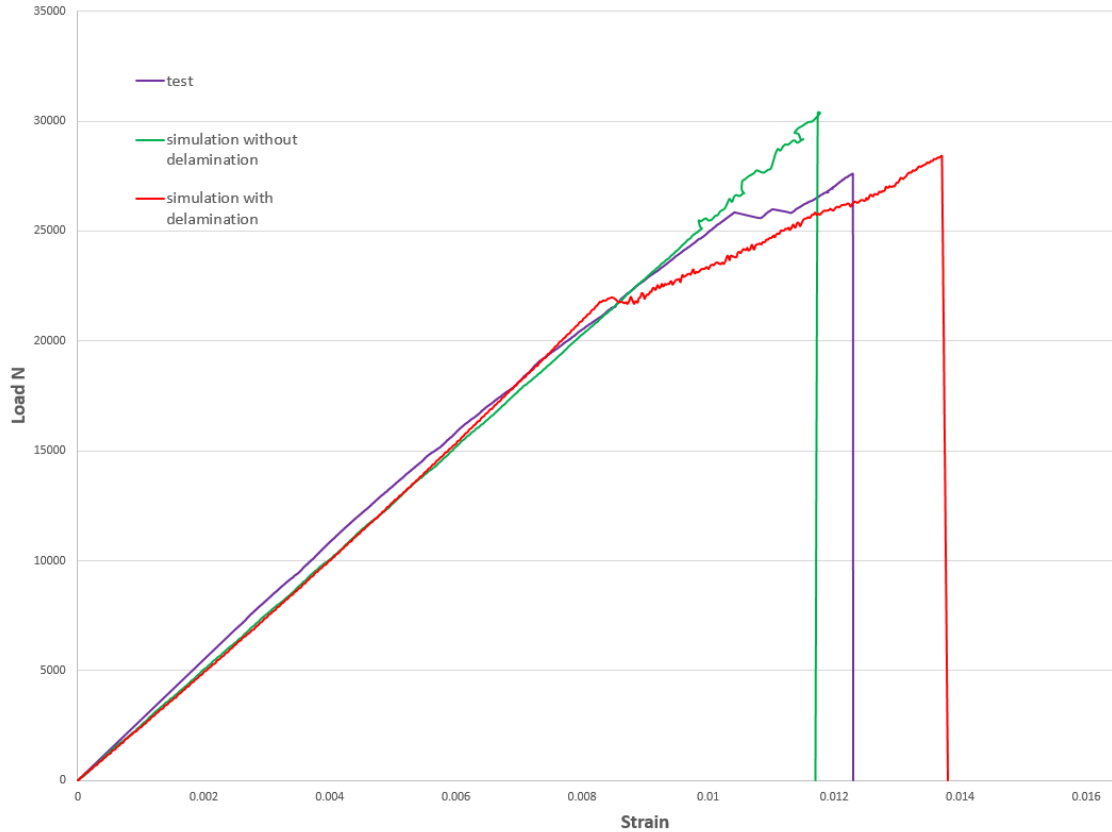


Figure 9. Load versus strain of OHT specimens (experiment and simulation)

Lay-up 2 - (22.5/67.5/-22.5/-67.5/-67.5/-22.5/67.5/22.5)

The lay-up considered in this section of the study is obtained by rotating the quasi-isotropic lay-up considered in the previous section by 22.5° . The open-hole test samples were prepared following ASTM standards and tested in tension using an Instron test apparatus. In Figure 10 the load versus strain measured for the OHT samples are presented. The average load measured at the final failure for this lay-up is around 22KN, whereas the experimental load measured for the lay-up-1 is at 29 KN. The stiffness of the composite with lay-up-2 is almost same as lay-up-1, but the load to the failure is lower by 30%. For the analysis of the composite with lay-up 2, the finite element model, the intra and inter-layer failure modeling, the material parameters, and analysis parameters were all the same as used in the analysis for lay-up 1 (except for the difference in fiber angles). Failed samples from the test are shown in Figure 11.

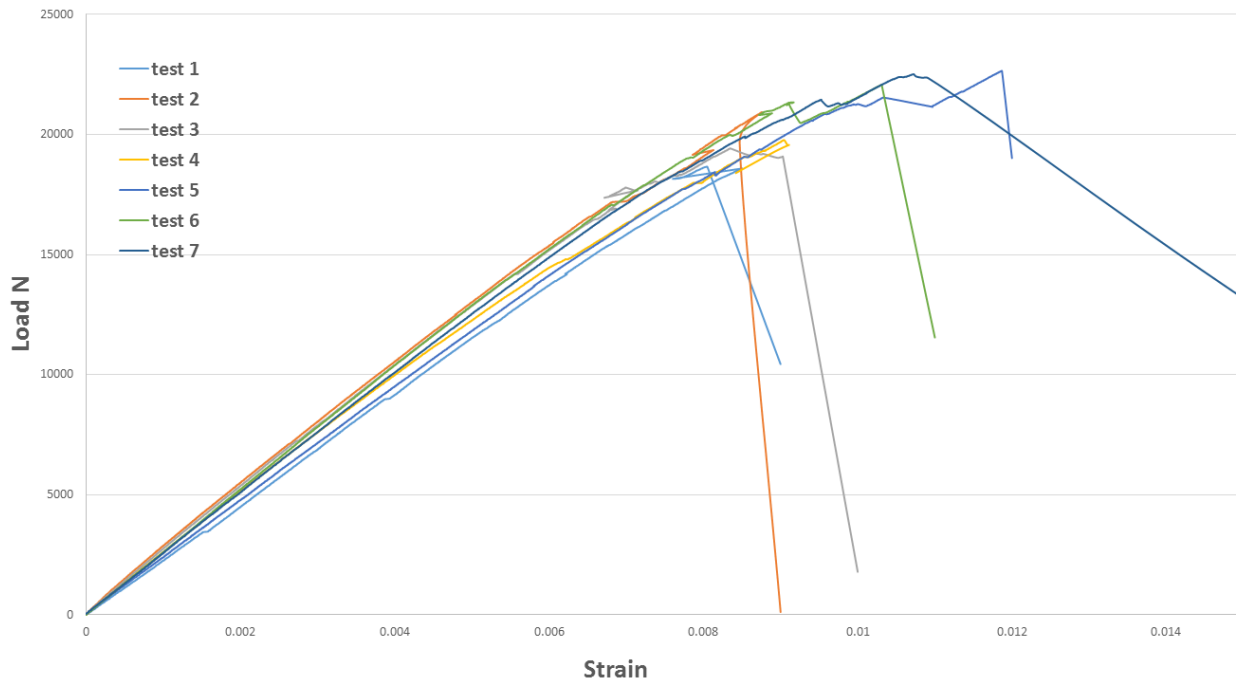


Figure 10. Experimental load versus strain for the OHT specimen with lay-up (22.5/67.5/-22.5/-67.5/-67.5/-22.5/67.5/22.5)

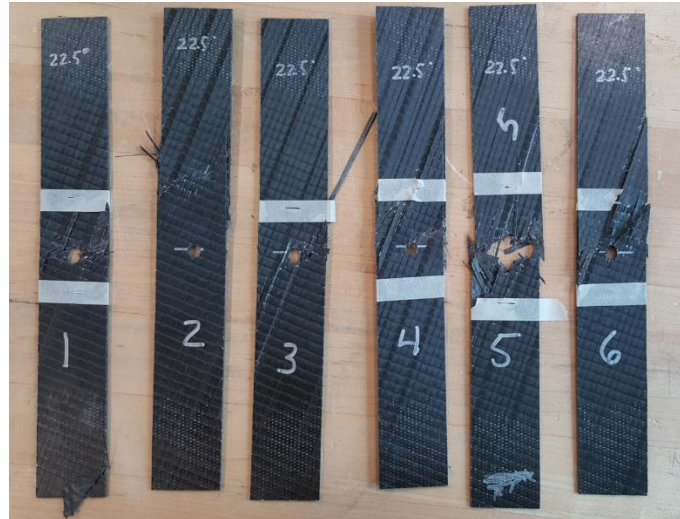


Figure 11. Failed samples of open-hole tension test (Lay-up 2)

In Figure 12 the load versus strain plotted from the test 5 experiment and the simulation are shown. The test 5 result, which was close to the mean response of the test samples, was used for comparison with the simulation results with and without delamination model. In general, a good agreement was observed between the simulation with delamination model and the experimental results. At a load of approximately 15 KN, the simulation predicts a deviation from linear behavior

and this could be due to the start of delamination damage in the specimen. Also, this trend was noticed in the experimental results too.

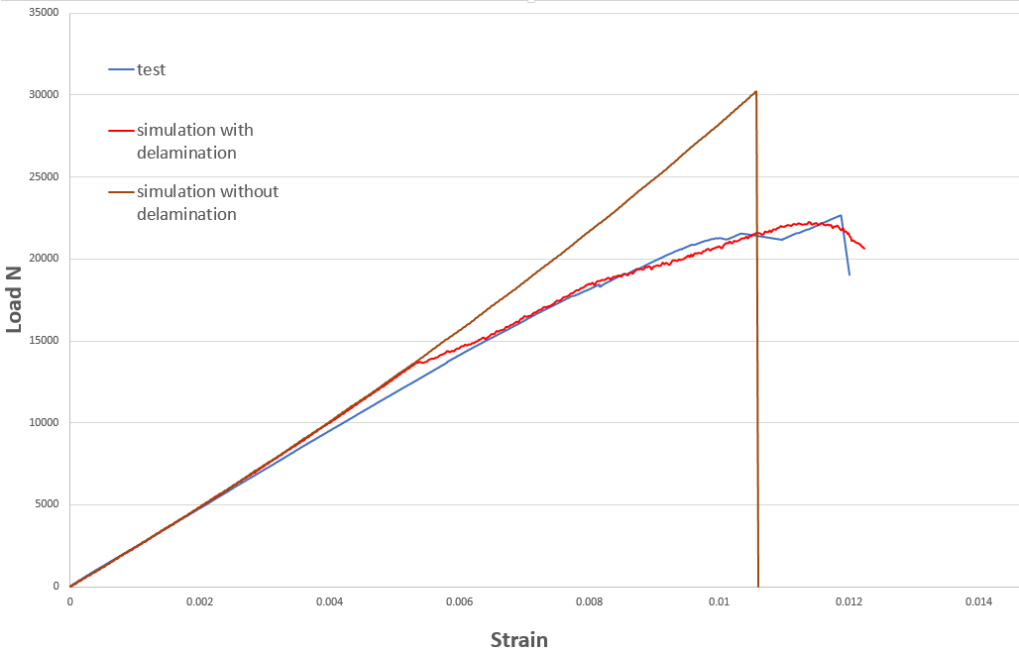
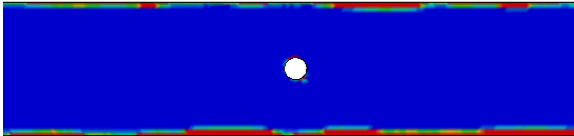
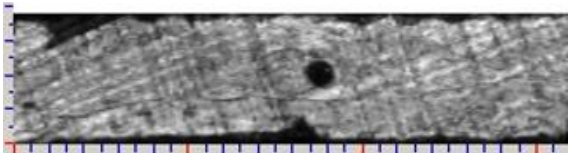


Figure 12. Experimental load versus strain for the OHT specimen with lay-up (22.5/67.5/-22.5/-67.5/-67.5/-22.5/67.5/22.5)

To verify further the reliability of inter and intra-layer damage modeling, the inter-layer damages at load level of 19 KN were obtained and compared with the simulation results in Figure 12. The delamination damage regions predicted from the simulation were denoted with red and the C-scan NDE delamination results with black.



a) Delamination results from simulation (red area) at the load of 19 KN



b) C-scan results of the experimental sample at the load of 19 KN

Figure 12. Delamination damage comparison between simulation and experiment at 19 KN

Figure 13 shows the delamination predicted in the sample just before the final failure. The delamination damage regions are indicated with red. Compared to the lay-up1, this lay-up experienced significant delaminations in the experiment and thus explains the load reduction compared to the lay-up 1.

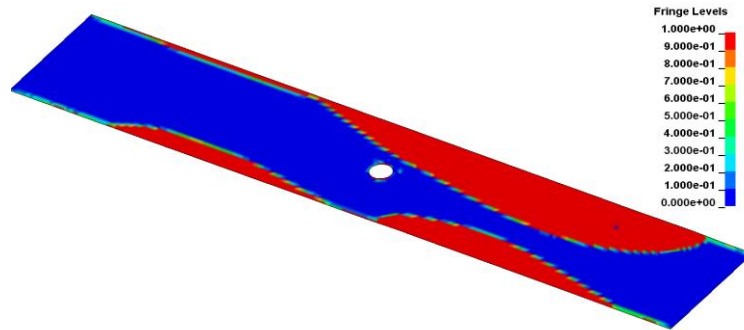


Figure 13. Delamination predictions for the OHT sample before the failure (lay-up 2)

From the correlations presented in Figure 11 and 12, one can see that the developed model for the intra and inter-layer modeling is able to provide good predictions for the failure load and delamination damage for the notched composites.

CONCLUSIONS

A Progressive damage model based on a continuum damage mechanics approach for intra-layer failure models for notched composites was developed and implemented in the LS-DYNA framework. The inter-layer damage was modeled using a tie break contact model available in LS-DYNA. The intra-laminar model exhibited mesh sensitivity and this spurious behavior was remedied by appropriately scaling the strength of the composite for various mesh densities. Mesh objectivity of the damage model was demonstrated by approximately simulating the same failure loads from four varying element size finite element models. Further, the model was validated by simulating failure loads and damage modes in open-hole tension experiments for two different lay-up configurations. One of the lay-ups considered in the study showed significant delamination near the free edges, providing a case with both inter and intra damages and the simulation model was able to predict this behavior with good accuracy.

REFERENCES

1. Waddoups, M.E., Eisenmann, J.R., Kaminski, B.E., 1971, "Macroscopic fracture mechanics of advanced composites materials", *J. Composite Materials*, Vol 5, pp 446-454.
2. Green, B.G., Wisnom, M.R., Hallet, S.R., 2007, "An experimental investigation into the tensile strength scaling of notched composites", *Composites – Part A*, Vol 38, pp 867-878.
3. Wisnom, M.R., Hallett, S.R., 2009, "The role of delamination in strength, failure mechanism and hole size effect in open hole tensile tests on quasi-isotropic laminates", *Composites A: Appl. Sci. Manuf.* Vol **40**, pp 335–342.
4. Satyanarayana, A., Bogert, P., Chunchu, P. B., "The Effect of Delamination on Damage Path and Failure Load Prediction for Notched Composite Laminates", 48th AIAA/ASME/ASCE/AHS/ASC Structures, Structural Dynamics and Materials Conference, AIAA 2007-1993, Honolulu, Hawaii.
5. Caminero, M.A., Lopez-Pedrosa, M., Pinna, C., Soutis, C., 2014, "Damage assessment of composite structures using digital image correlation", *Appl. Composite Materials*, Vol 21, pp 91–106.
6. Whitney, J.M., Nuismer, R.J., "Stress fracture criteria for laminated composites containing stress concentrations", *J. Composites Materials*, Vol 8, pp 253-265.
7. Pipes, R.B., Wetherhold, R.C., and Gillespie, J.W., 1979, "Notched Strength of Composite Materials", *J. Composite Materials*, Vol 13, pp 148-160.
8. Rice, J.R., 1968, "A Path Independent Integral and the Approximate Analysis of Strain Concentration by Notches and Cracks", *J. Applied Mechanics*, Vol 35, No. 2, pp 379-386.
9. Satyanarayana, A., Bogert, P., Karayev, K., Nordman, P.S., Razi, H., 2012, "Influence of finite element size in residual strength prediction of composite structures", 53rd AIAA/ASME/ASCE/AHS/ASC Structures, Structural Dynamics and Materials Conference, AIAA 2012-1619, Honolulu, Hawaii.
10. Kenik, D., Nelson, E.E., Robbins, D., Mabson, G., 2012, "Developing guidelines for application of coupled fracture/continuum mechanics – based composite damage models for reducing mesh sensitivity", AIAA/ASME/ASCE/AHS/ASC Structures, Structural Dynamics and Materials Conference, Honolulu, Hawaii.
11. Bazant, Z.H., and Oh, B.H., 1983, "Crack-band theory for fracture of concrete", *Materials and Structures*, Vol 16, pp 155-177.
12. Aitharaju, V., Aashat, S., Kia, H., Satyanarayana, A., Bogert, P., 2015, "Axial crush and bending collapse analysis of non-crimped fabric composite structures", *Proceedings of American Society for Composites 30th technical conference*.

